for each i. These annuli are specified in the standard model of a generalized tower, built using standard blocks. Note that the attaching circle is contained in the spine.

Next we restrict to the special types of generalized towers that we will wish to construct in the upcoming proof. In the course of their construction, other generalized towers will arise, so it will be useful to have defined the generalized objects of Definition 12.5.

Definition 12.6

(1) A *grope* $G(h)$ of height h is a symmetric generalized tower of height h with only surface stages. The spine of a grope is sometimes called a 2-dimensional grope by other authors. See Figure 12.3 and Remark 12.7, compare with Section 5.1.2.

(2) A *capped grope* $G^c(h)$ of height h is a symmetric generalized tower of height $h+1$ where the stages $G_1, \dots, G_h$ are surface stages and G_{h+1} is a cap stage. The union of the constituent surface stages is called the *body* of the capped grope. See Figure 12.4.

(3) A *tower* $\mathcal{T}_n$ with n storeys is a symmetric generalized tower $G_0 \cup G_1 \cup \cdots \cup G_h$, where each $\mathcal{G}_i = (G_i, \Sigma_i, \Phi_i, \Psi_i)$ for $i \geq 1$ is either a surface or disc stage, and such

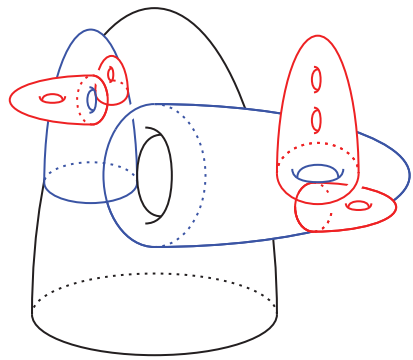

Figure 12.3 Schematic picture of the 2-dimensional spine of a height three grope.

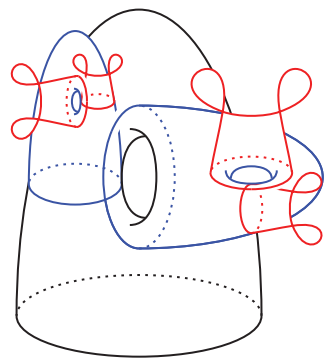

Figure 12.4 Schematic picture of the 2-dimensional spine of a height two capped grope.

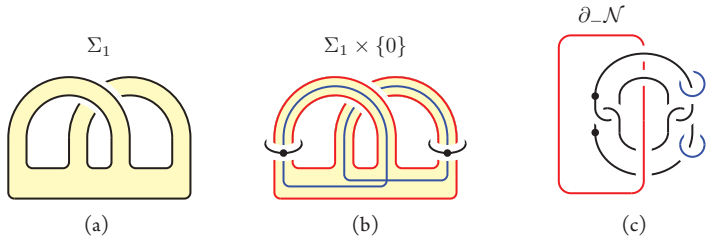

Figure 13.10 (a) The surface Σ_1 (yellow) is produced by attaching a pair of 2-dimensional 1-handles to a 2-dimensional 0-handle. (b) By taking the product of the handle decomposition in (a) with D^2, we obtain a (4-dimensional) handle decomposition of $\Sigma_1 \times D^2$. The handle decomposition consists of the pair of 1-handles denoted by the two dotted circles, attached to a 0-handle. The surface $\Sigma_1 \times \{0\}$ is shown in yellow with red boundary. A symplectic basis of curves for $H_1(\Sigma_1 \times \{0\})$ is shown in blue. (c) The result of an isotopy of the Kirby diagram in (b). The red circle is the image of the boundary of $\Sigma_1 \times \{0\}$. This is a Kirby diagram for a surface block $\mathcal{N}$ with genus one. The attaching region $\partial_- \mathcal{N}$ is a trivially framed, tubular neighbourhood of the red circle, while the tip region consists of trivially framed, tubular neighbourhoods of the blue circles.

block is pictured in Figure 13.10(b). As a sanity check, note that, as expected, $\Sigma_1 \times D^2$ is diffeomorphic to $S^1 \times D^3 \natural S^1 \times D^3$.

To understand the framing of the attaching and tip regions, we recall the definition of the abstract surface block from Chapter 12 in greater detail. Begin with a standard surface in S^3 with a single boundary component, thicken first within S^3, and then again by multiplying the model with $[0, 1]$. The framing of the attaching circle is obtained from the tangent vectors to the two thickenings. Since the first thickening takes place within S^3, the framing is the Seifert framing. The framing of the tip regions is given by the surface framing and the second thickening direction. From Figure 13.10(b), this is also seen to be the Seifert framing.

More generally, one can follow the same procedure starting with a decomposition of Σ_g into $2g$ 1-handles attached to a 0-handle, for any $g \geq 1$. In this case, we obtain a Kirby diagram for a surface block of genus g, as indicated in Figure 13.11. Again the attaching region is given by a trivially framed neighbourhood of the red circle, while the tip region consists of trivially framed neighbourhoods of the blue circle.

13.4.2 Disc and Cap Blocks

Recall that disc and cap blocks both consist of self-plumbed thickened discs. In the language of this chapter, these are self-plumbed 2-handles. They are not yet attached to any 4-manifold, but the attaching region records how they should be attached. From Section 13.3.3, we see that Figure 13.12 depicts a Kirby diagram for a self-plumbed 2-handle. In particular, the 4-manifold is the boundary connected sum $\natural^n S^1 \times D^3$ for some n, as expected. In a disc block the number of positively and negatively clasped dotted circles must match up, and the meridians of these dotted circles form the tip regions. In a cap block, there is no restriction on the signs of the clasps of the dotted circles and there are no tip regions.

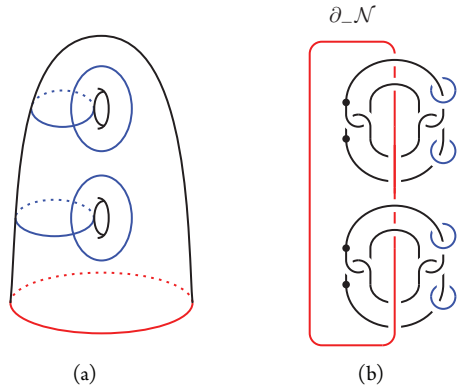

Figure 13.11 (a) The abstract surface Σ_2 with boundary shown in red and a symplectic basis of curves for $H_1(\Sigma_2;\mathbb{Z})$ shown in blue. (b) A Kirby diagram for the surface block $\mathcal{N}$ with genus two. The attaching region $\partial_- \mathcal{N}$ is a trivially framed neighbourhood of the red circle. The tip region consists of trivially framed neighbourhoods of the blue circles.

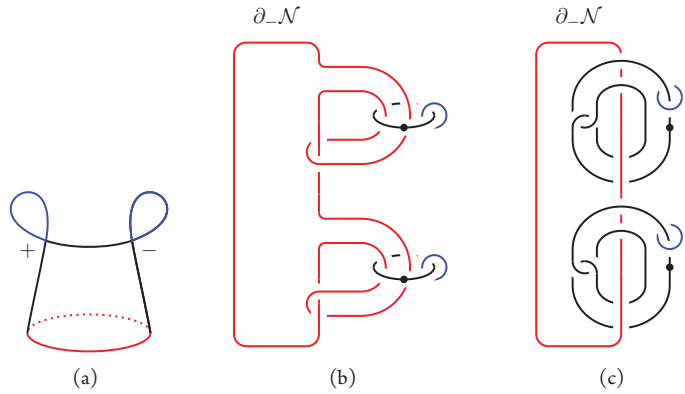

Figure 13.12 (a) A schematic picture of the 2-dimensional spine of a disc block with one positive and one negative self-plumbing. (b) A Kirby diagram for the disc block indicated in (a). The attaching region $\partial_- \mathcal{N}$ is a trivially framed neighbourhood of the red curve and the tip region consists of trivially framed neighbourhoods of the blue curves. Note that if we forget the tip regions, this is also a Kirby diagram for a cap block. (c) The result of an isotopy on the diagram in (b).

Next we describe the spine of the disc and cap blocks. Let $\mathcal{N}$ be a disc or cap block with underlying 4-manifold N. Following Section 13.3.3, the spine of $\mathcal{N}$ is an immersed disc in N with transverse self-intersections in the interior, seen in Figure 13.12(b), as follows. There is a homotopy of the attaching circle in the complement of the dotted circles consisting of crossing changes, taking it to an unknotted circle split and unlinked from the dotted circles. That is, the result of the homotopy bounds a disc away from the dotted circles. The trace of the homotopy glued to this disc is the spine of $\mathcal{N}$.

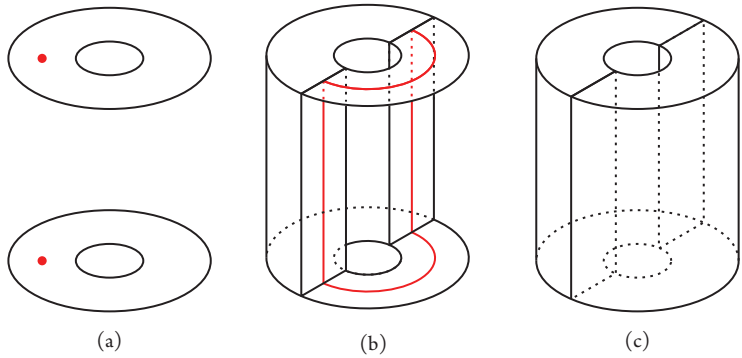

Figure 13.13 (a) Two copies of $S^1 \times D^2$ to be identified. The third dimension is suppressed. The attaching sphere for a 1-handle is indicated in red. (b) After attaching a 1-handle. The attaching circle for a 2-handle is shown in red. (c) A copy of $S^1 \times D^2 \times [0,1]$ has been constructed.

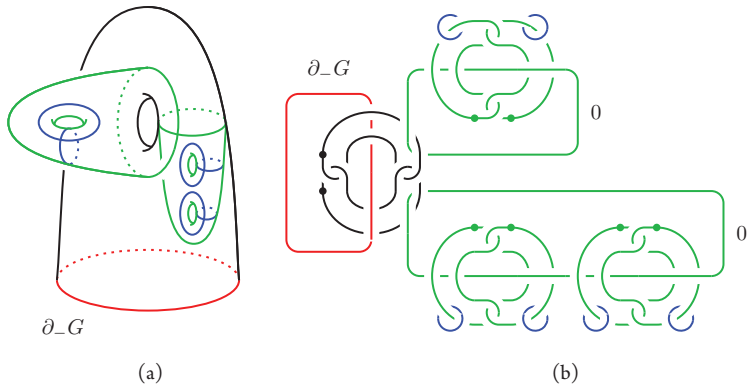

Figure 13.14 (a) The 2-dimensional spine of a height two grope, G. Tip circles are shown in blue. (b) A Kirby diagram for the grope indicated in (a). The attaching region ∂_G is a trivially framed neighbourhood of the red circle. The second stage surfaces are shown in green in both panels. The tip region consists of trivially framed neighbourhoods of the blue circles.

In practice, if a block $\mathcal{N}_2$ is to be stacked on top of a block $\mathcal{N}_1$, we place the Kirby diagrams next to each other, take the connected sum of the curves denoting the corresponding tip and attaching regions, and declare the resulting curve to be a 2-handle attaching circle. Since the attaching and tip regions were trivially framed, the new curve is also trivially framed. The result is a Kirby diagram for the manifold produced by stacking $\mathcal{N}_2$ on top of $\mathcal{N}_1$, as desired. We illustrate this procedure with a number of pictures, in Figures 13.14–13.16.

Using the procedure just described, the reader should now be able to draw Kirby diagrams for arbitrarily complicated generalized towers. However, as exemplified in particular by Figure 13.16, these diagrams rapidly increase in complexity as the number of stages increases. We will soon see how to simplify these diagrams.

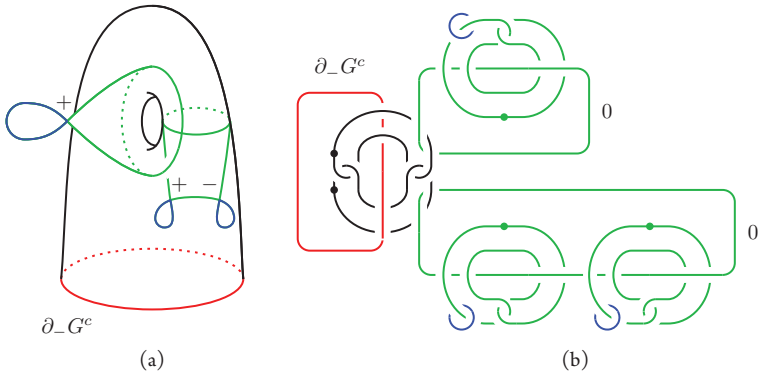

Figure 13.15 (a) The 2-dimensional spine of a height one capped grope G^c. (b) A Kirby diagram for the capped grope indicated in (a). The attaching region ∂_G^c is a trivially framed neighbourhood of the red circle. The caps are shown in green in both panels. The tip region consists of trivially framed neighbourhoods of the blue circles.

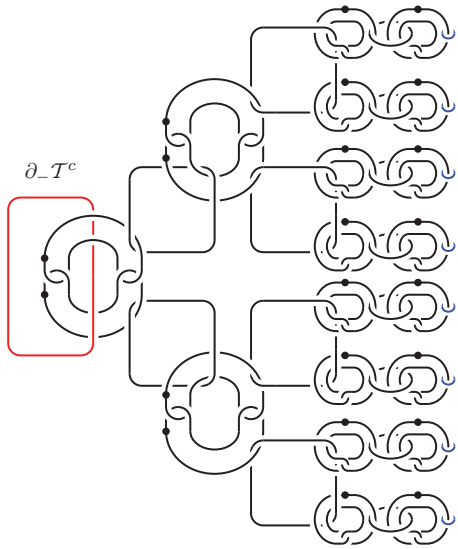

Figure 13.16 A Kirby diagram of a 1-storey capped tower $\mathcal{T}^c$. All solid black curves without dots are 0-framed by default. The attaching and tip regions are trivially framed neighbourhoods of the red and blue circles, respectively, as usual. We invite the reader to draw an abstract picture of the 2-dimensional spine of $\mathcal{T}^c$.

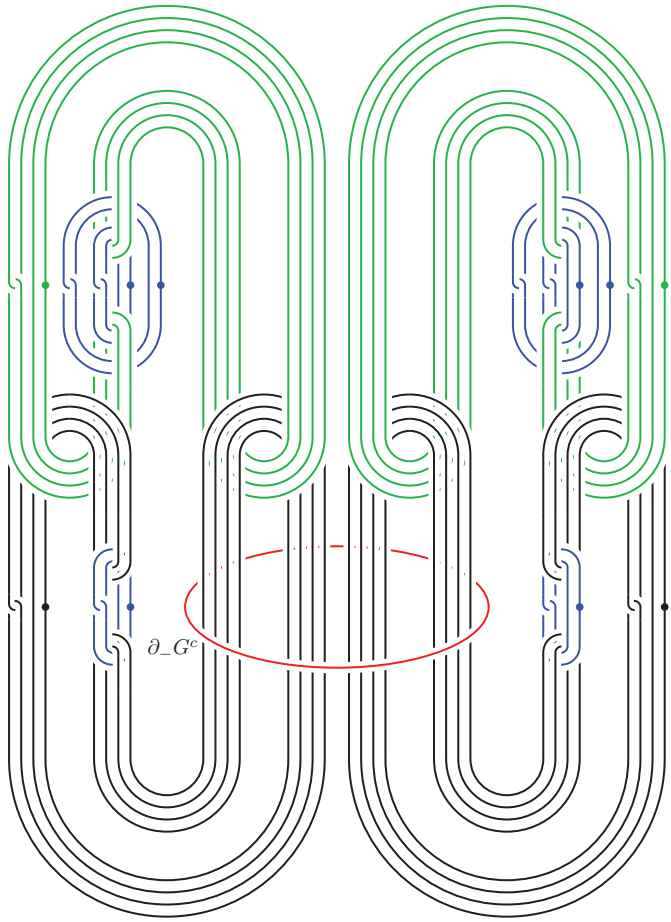

Figure 13.23 A Kirby diagram for a height two capped grope G^c, illustrating some nontrivial ramification. The attaching region $\partial_- G^c$ is a trivially framed neighbourhood of the red circle. We invite the reader to determine the 2-dimensional spine of G^c and to determine where the tip region lies in this diagram.

13.7 Chapter Summary

We repeat the key points the reader should recall from this chapter moving forward. First of all, we have constructed Kirby diagrams for towers, consisting only of dotted circles. This implies that every tower or capped tower is diffeomorphic to a boundary connected sum $\natural^m S^1 \times D^3$ for some m. By the interpretation of the dotted circle notation for 1-handles given in Section 13.2.1, towers can be understood explicitly as a subset of D^4. More precisely, let $\{\Delta_i\}$ denote the collection of standard unknotted, disjointly embedded discs in D^4 bounded by the dotted circles in the (simplified) Kirby diagram for the tower. Then

other arcs. At the end of the process, all Whitney arcs are mutually disjoint. From now on, we always assume that Whitney circles are disjoint without comment or loss of generality.

Remark 15.1 The last two techniques show how to complete the proof of Proposition 11.10. In that proposition, we obtained immersed Whitney discs using algebraic topological considerations, due to the vanishing of the appropriate intersection and self-intersection numbers. These discs come from null homotopies and thus they may not *a priori* be framed. The boundary twisting operation allows us to ensure that the Whitney discs are framed, at the expense of adding new points of intersection between the Whitney discs and the original surfaces. Since such intersections are often already present, or at least cannot be assumed not to be present, this does not hurt us in practice. The boundary of the Whitney discs may not be embedded or mutually disjoint to begin with, but this can be ensured by the procedure of this section and we will occasionally assume this without comment.

15.2.4 Pushing Down Intersections

The technique of pushing down intersection points was introduced in [FQ90, Section 2.5]. Suppose we have two immersed surfaces A and B such that part of the boundary of B is embedded in A, as shown on the left of Figure 15.6 (note this is the same situation as in Figure 15.4). Then any intersection between B and some third surface C can be removed at the expense of adding two new intersections between C and A. This is shown on the right of Figure 15.6. For us, most often A will be part of a surface stage in a capped grope or tower, and B will be part of either a cap stage or a surface stage. We can then iteratively push down intersections with B to any surface stage including or below A. One advantage of doing this is that the new intersections appear in algebraically cancelling pairs and thus have associated Whitney discs. Alternatively, often a lower stage of a grope will have a geometrically transverse sphere, and so we can push down the intersection points and then tube the many new intersection points into the geometrically transverse sphere.

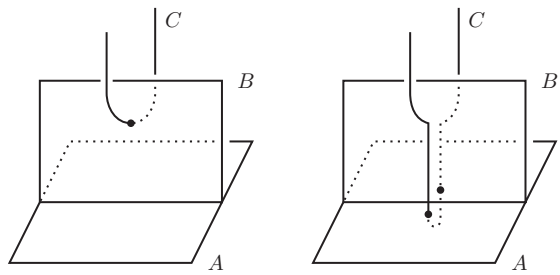

Figure 15.6 Pushing down an intersection point between C and B (left) leads to two new intersection points between C and A (right). Note that the two new intersection points are evidently paired by an embedded, framed Whitney disc. Only a single time slice is pictured. Note that we are performing a finger move, albeit one that pushes across the boundary and therefore does not preserve intersection numbers.

15.2.5 *Contraction and Subsequent Pushing Off*

Contraction and push-off was introduced in [FQ90, Section 2.3]. The (symmetric) contraction of a capped surface, depicted in Figure 15.7, converts a capped surface into an immersed disc. As shown by the figure, we start with a symplectic basis of curves on the surface and surger the surface using two copies each of framed immersed discs bounded by these curves joined by a square at the point of intersection of the curves. One could, alternatively, contract a capped surface by only surgering along one disc per dual pair, but this would not enable the pushing off procedure that we are about to describe in the next paragraph. Henceforth, whenever we talk about contraction, by default we will mean the symmetric contraction. Observe that the result of contracting a capped surface with embedded body has algebraically cancelling self-intersections.

After contracting a capped surface Σ^c with body Σ, any other surface A that intersected the caps of Σ^c can be pushed off the contracted surface, as we describe in Figure 15.8. The fact that we can perform the pushing off procedure, which is a regular homotopy, shows that the intersection number of the contracted surface with A is trivial. The push-off procedure reduces the number of intersection points between the contracted surface (an immersed disc) and the pushed off surfaces, so we gain some disjointness at the expense of converting a capped surface into an immersed disc. An additional cost is as follows. Suppose that a surface A intersects a cap of the capped surface, and a surface B intersects a dual cap. Then after pushing both A and B off the contraction, we obtain two intersection points between A and B. The contraction push-off operation is shown, via before and after pictures, in Figure 15.8.

A useful observation is that the homotopy class of the surface resulting from a contraction of a capped surface is independent of the choice of caps.

Lemma 15.2 *The homotopy class of the sphere or disc resulting from symmetric contraction of a fixed capped surface is independent of the choice of caps, provided the boundaries of the different choices of caps coincide.*

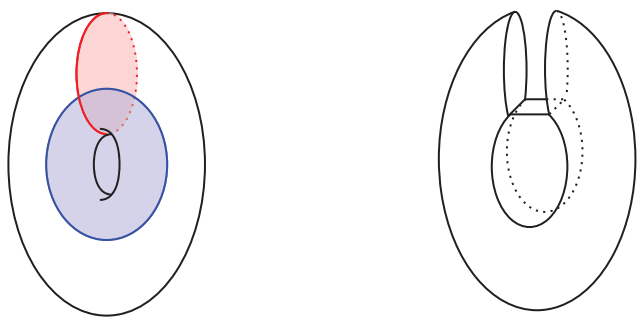

Figure 15.7 (Symmetric) contraction of a capped surface. Here we show the situation for embedded caps.

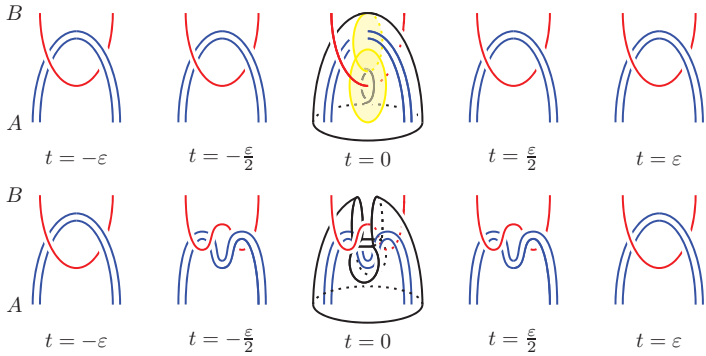

Figure 15.8 Top: Before contraction of a surface. Bottom: After contraction, with other surfaces pushed off the result of contraction. The capped surface being contracted is shown in the middle time slice. The surfaces A and B being pushed off the contraction are shown in blue and red, respectively. Note that the intersections of the pushed-off surfaces occur between diagrams one and two and between diagrams four and five in the bottom row of figures, namely one intersection in the past and one intersection in the future between each pair of surfaces that were pushed off dual caps.

Proof As explained in [FQ90, Section 2.3], an isotopy in the model capped surface induces a homotopy of the immersed copies. In the model, the symmetric contraction along dual caps $\{C, D\}$ is isotopic to the result of surgery along either cap; for example, C. This can be seen directly by isotoping across the region lying between the parallel copies of D used in the symmetric contraction (see Figure 15.7). Therefore, once the model is immersed in a 4-manifold, the symmetric contraction is homotopic to the result of surgery along one cap per dual pair.

Now let $\{C_i, D_i\}_{i=1}^g$ and $\{C_i', D_i'\}_{i=1}^g$ be two sets of caps for a surface of genus g such that $\partial C_i = \partial C_i'$ and $\partial D_i = \partial D_i'$ form a dual pair of curves on the surface for each i. Then the result of contraction along $\{C_i, D_i\}_{i=1}^g$ is homotopic to the asymmetric contraction along $\{C_i\}$, which is homotopic to contraction along $\{C_i, D_i'\}_{i=1}^g$. This is, in turn, homotopic to the result of asymmetric contraction along $\{D_i'\}$, which finally is homotopic to the result of contraction on $\{C_i', D_i'\}_{i=1}^g$, as asserted. □

15.3 Replacing Algebraic Duals with Geometric Duals

We finish the chapter with two applications of the techniques introduced so far. The first lemma will be used repeatedly in the upcoming constructions. It allows us to improve algebraic duals into geometric duals, at the cost of introducing new self-intersections, and first appeared in this form in [Fre82a, Lemma 3.1]. Compare with the techniques described in Chapter 1 and see also [FQ90, Section 1.5].

We leave it to the reader to determine the correct definition for when $m \in \frac{1}{2}\mathbb{N}$ and $\mathcal{A}$ and $\mathcal{B}$ are asymmetric generalized towers.

Here is the precise statement of grope height raising. This applies to both union-of-discs-like and union-of-spheres-like gropes.

Proposition 17.3 (Grope height raising) *Given a union-of-discs-like or union-of-spheres-like capped grope $G^c(m)$ of height $m \in \frac{1}{2}\mathbb{N}$, where m is at least 1.5, and a positive integer $n \geq m$, there exists a capped grope $G^c(n)$ of height n embedded in $G^c(m)$ such that the first m stages of $G^c(n)$ and $G^c(m)$ coincide.*

Moreover, any collection of geometrically transverse capped gropes or spheres for $G^c(m)$ is also geometrically transverse to $G^c(n)$.

The proof of grope height raising will combine the following two results.

Lemma 17.4 (Cap separation lemma) *Given an asymmetric union-of-discs-like or union-of-spheres-like capped grope $G^c(m)$ of height (a, b), where $a \geq 1$, there exists a capped grope embedded in $G^c(m)$, with the same height, body, and attaching region as $G^c(m)$, such that its $(+)$-side caps are disjoint from its $(-)$-side caps.*

This lemma first appeared in print in [CP16].

Proof First we construct a union-of-spheres-like capped grope T^c_- such that its body T_- and the $(-)$-side $G^c(m)^-$ of $G^c(m)$ are geometrically transverse. Note that $G^c(m)^-$ might consist only of caps. Take two parallel push-offs of the $(+)$-side grope $G^c(m)^+$. The induced push-offs of the attaching circles of the $(+)$-side grope $G^c(m)^+$ are connected by annuli which intersect the bottom stage of the $(-)$-side grope $G^c(m)^-$ once transversely, as shown in Figure 17.2. Let T^c_- be the union of the two parallel push-offs and the corresponding annuli. By construction, we see that the body of the union-of-spheres-like grope T^c_- and the $(-)$-side grope $G^c(m)^-$ are geometrically transverse, while the caps of T^c_- may

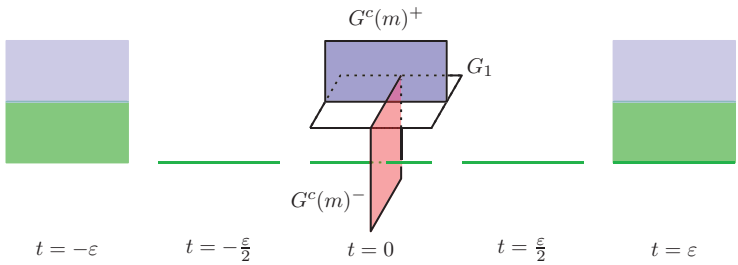

Figure 17.2 We show a local picture for the attaching circle of a single component of the body of the $(+)$-side $G^c(m)^+$ (blue) to a first stage surface G_1 of $G^c(m)$. The $(-)$-side is shown in red. Lighter blue depicts the two parallel push-offs of the $(+)$-side, while green indicates an annulus connecting the two push-offs of the attaching circle. Note the single transverse intersection between the annulus and the $(-)$-side in the central image.

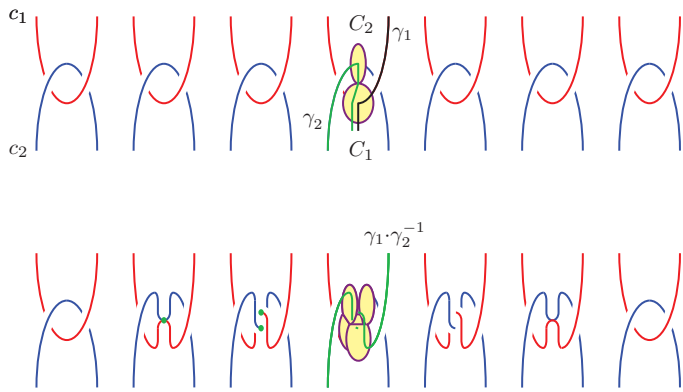

Figure 19.1 New double point loops after a contraction followed by push-off. We do not draw the surface being contracted in the figure. Compare with Figure 15.8.
Top: Dual caps C_1 and C_2 are shown in yellow. The caps c_1 and c_2 are shown in red and blue, respectively. Black and green show pieces of the double point loops γ_1 and γ_2 for the intersection point between C_1 and c_1 and the one between C_2 and c_2, respectively.
Bottom: Green shows a piece of a new double point loop. Most of the piece shown is in the middle panel, but there is a (trivial) finger extending backwards in time, with the peak at the new double point. A similar extension to the right, which we do not show, would give the double point loop for the second new intersection point, which is visible in the second image from the right.

designated as first. Push off caps at any intersections whose double point loops were mapped by ϕ to γ_n. Make sure to push the first sheet off the second. The new grope still has a map from its fundamental group to Γ. By Lemma 19.1, the new intersections created by pushing off in this step have double point loops given by $\gamma_n \cdot \gamma_n^{-1}$; that is, they are mapped to the trivial element in Γ.

Now perform this process iteratively: at the ith step, contract the $(n+1-i)$th stage of the capped grope, assign first and second sheets as before, then push off intersections mapped by $\phi\colon \pi_1(G') \to \Gamma$ to γ_{n+1-i}. After contracting the n stages of G', we are left with an immersed disc D whose framed boundary coincides with the attaching region of G' and thus G, such that all the double point loops are mapped to the identity element of Γ. This completes the proof. □

Before proving that the infinite cyclic group is good, we investigate the behaviour of double point loops under the operation of grope height raising.

Lemma 19.3 *Let G be a height 1.5 disc-like capped grope. For any $i \geq 0$, there exists a height 2^i capped grope G', contained within G with the same attaching region, such that each double point loop of G' has length at most 7^{2i} in the double point loops of G.*

Proof We recall the proof of grope height raising (Proposition 17.3). It alternates raising the height of the $(+)$- and $(-)$-sides of G. Start with the $(-)$-side, which consists only of caps at the beginning. First, we use the cap separation lemma (Lemma 17.4) to make the $(+)$-side and $(-)$-side caps disjoint. This changes the $(-)$-side caps of G by a push-off operation. By

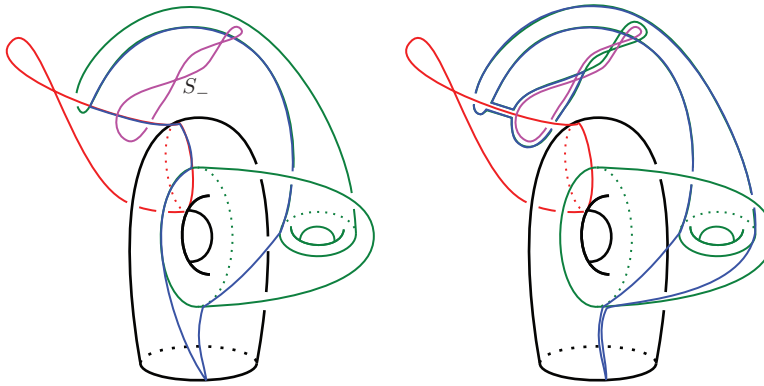

Figure 19.2 (a) We see a disc-like capped grope of height 1.5, after the first step of the cap separation lemma. More precisely, parallel copies of the $(+)$-side (green) have been used to produce a sphere S_- (pink), geometrically transverse to the $(-)$-side (red). We only show a single $(+)$-side cap. The $(+)$-side cap intersects the $(-)$-side cap. The double point loop for the intersection point is shown in blue.
(b) The intersection point between the $(+)$- and $(-)$-side cap has been removed by tubing into S_-. The double point loop for the new $(+)$-side intersection point is shown in blue. Note that it passes through an intersection of S_- (arising from an intersection point of the $(+)$-side), as well as the old intersection point between the $(-)$- and $(+)$-side caps. More precisely, the double point loop is a conjugate of a double point loop for a $(+)$-side intersection point by a double point loop for an intersection between $(-)$- and $(+)$-side caps.

Lemma 19.1, each new intersection point has a double point loop given by the product of two double point loops of previous intersections.

The $(+)$-side caps also change during cap separation. As shown in Figure 19.2, each double point loop is changed by conjugation by a double point loop.

Then we produce geometrically transverse union-of-spheres-like gropes for the $(-)$-side by using parallel copies of the $(+)$-side grope, which has height one at the beginning. Next, tube the intersections among the $(-)$-side caps into this grope (after first pushing down to the bottom stage of the $(-)$-side if necessary). The $(-)$-side caps now become capped gropes, which are still on the $(-)$-side by definition. Since parallel copies of the $(+)$-side caps were used in this process, the new $(-)$-side caps now intersect the $(+)$-side caps. From Figure 19.3, we see that a double point loop for a new intersection between a $(+)$-side cap and a $(-)$-side cap goes through two old intersections; these have length five in terms of double point loops of the original grope. Similarly, a double point loop for a new intersection between two $(-)$-side caps goes through three old intersections, two of which are produced by contraction and push-off operations; these have length seven in terms of double point loops of the original grope.

Putting all of the previous steps together, we see that each of the final double point loops can be written as a product of at most seven double point loops of the original grope.

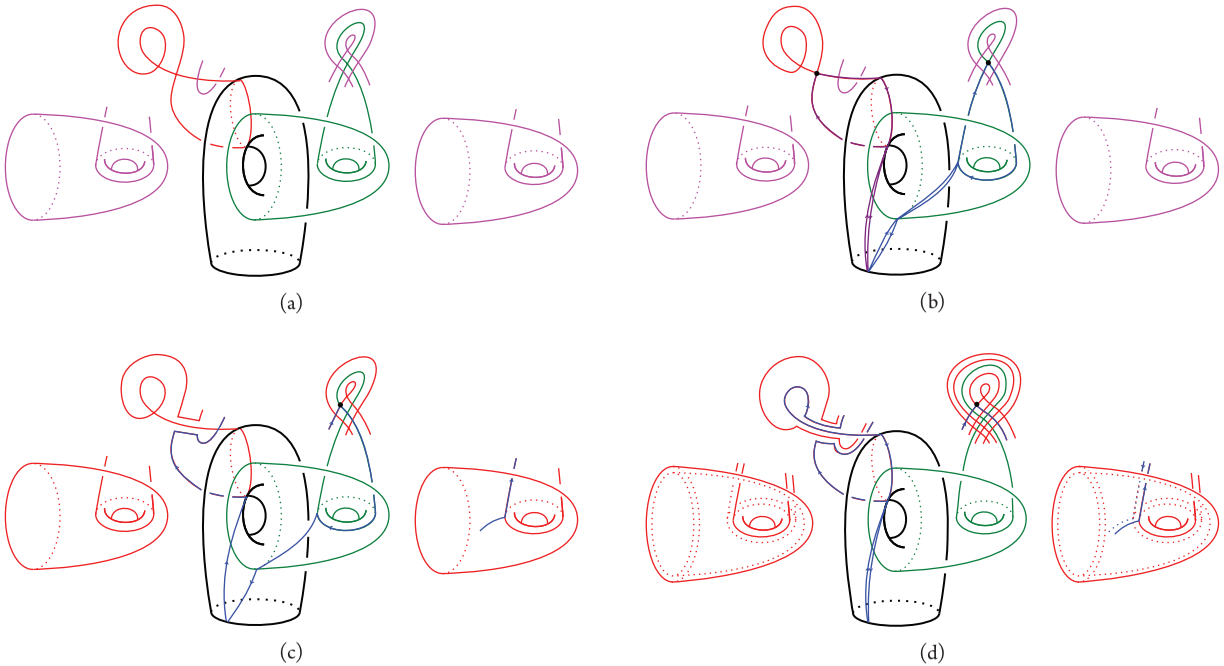

Figure 19.3 (a) A disc-like capped grope of height 1.5 after cap separation, divided into a $(-)$-side (red) and a $(+)$-side (green). The transverse sphere-like grope (pink) for the $(-)$-side cap includes an annulus joining the two parallel copies of the $(+)$-side. (b) Double point loops (purple and blue) for a $(-)$-side and $(+)$-side cap intersection. (c) After tubing a $(-)$-side cap intersection into the transverse grope, a new intersection between the new $(-)$-side cap and a $(+)$-side cap is created, with a (blue) double point loop. (d) After tubing two $(-)$-side cap intersections into the transverse grope, a new intersection between $(-)$-side caps is created, with a blue double point loop.